Journal of Current Veterinary Research

ISSN: 2636-4026

Journal homepage:http://www.jcvr.journals.ekb.eg

Surgery

The Efficacy of Nano-Calcium Carbonate Derived from Coral Reefs and Nano-Silver to Induce new bone formation in Critical Radial Bone Defect in Rabbits: Radiological Evaluation

Gadallah Shaaban M., Mohamed Abd-Elkawi*, Tarek N. Misk and Ahmed M. Sharshar

Department of Surgery, Radiology and Anesthesiology, Faculty of Veterinary Medicine, University of Sadat City.

**Corresponding author:* moh.abdelkawi@gmail.com *Received: 9/3/2022 Accepted: 2/4/2022*

ABSTRACT

This study aimed to evaluate the efficacy of calcium carbonate nanoparticles (CCNPs) and Silver nanoparticles (Ag NPs) to induce new bone formation and accelerate bone regeneration when be used to fill an experimentally critical defect in the radial bone of rabbits. 24 adult apparently healthy New Zealand white rabbits aged from 5-6 months and weighing 3.5 ± 0.5 kg were used in this study and were divided into two groups, group A: we used CCNPs paste only. Group B: we used CCNPs/Ag NPs paste. During the observation period, rabbits were observed clinically and radiographically at 2,4,8,12 weeks post-operation. *Results*: the total radiographic score showed that there was a significant difference between groups (A) and group (B) at the eighth postoperative week and at the period of observation (12 weeks) while there was no significant difference at second and fourth post an operative week. *Conclusion*: radiographical studies revealed that CCNPs and Ag NPs have the ability to induce new bone formation and CCNPs/AgNPs paste was able to make relatively complete healing at the end of the observation period.

Keywords: AgNPs, A-PRF, Bone healing, CCNPs and Nanoparticles.

INTRODUCTION

Bone tissue has the capacity for regeneration and remodeling, both processes are often impaired in many clinical situations including bone loss caused by diseases, trauma or tumors requiring transplantation of bone tissue substitution such as autograft, allograft ,mineral bone substitutes (as calcium carbonate, calcium phosphate,..etc), cell derived biomaterial (PRP, PRF, stem cells….etc) or nanomaterials (nano-silver, nano-zinc oxide). These substitutions are the most commonly used technique for skeletal reconstruction and accelerating bone regeneration in which spontaneous bone regeneration limitation is expected in these situations' resection(Esposito et al., 2010).

The ideal materials for bone fracture repair should possess the following six characteristics: (i) good biocompatibility. The material itself and its degradation products should be non-toxic. (ii) Appropriate biodegradability. The material should be able to degrade after fulfilling its targeted mission and its degradation rate should match the tissue growth rate. (iii) Optimal plasticity and mechanical properties. The material can be made into desired shapes and provide support for new tissue growth until the repair process is complete. (iv) Good osteo-inductivity and osteo-conductivity. The material is expected to induce osteogenesis and to stimulate bone growth. (v) A three-dimensional (3D) porous structure. The material is desirable if can be processed into a three-dimensional porous structure which mimics the structure of bones and is conducive for cell adhesion and

extracellular matrix deposition and has passages for nutrients and oxygen. (vi) Easily sterilized, while maintaining its mechanical and biological properties (Hak, et al., 2014).

Nanomaterials have shown improved bone cell functions compared to their micron-sized counterparts and have been emerging as a new viable class of materials for bone fracture repair. This is because nanomaterials may precisely mimic the hierarchical and nanoscale features of bones (Puska et al., 2013).

Corals belong to the phylum Cnidaria, and most belong to class Anthozoa. There are two types of coral, soft and hard (stony) coral, but only the hard one is used for bone tissue engineering. stony corals secrete an external calcium carbonate skeleton, which combined with an open, highly interconnected porous structure with pore sizes between 100 μm and 500 μm diameter with a high degree of connectivity, make them of interest as scaffolds for bone growth (Castro et al., 2008).CCNPs derived from Coral (stony coral) is used as bone graft substitute because its structure resembles the mineral structure of the normal bone, also it was easily prepared, cost effective and had no toxic effect on the animal model (Mahmood et al., 2017).

Nanosilver particles (AgNPs) generally present at 1 to 100 nm in size in at least one dimension (Mohamed et al., 2012 and Chen et al., 2013). As particle size decreases, the surface area-to-volume ratio of Ag NPs increases dramatically, which leads to significant changes in their physical, chemical, and biological properties. Ag NPs have been among the most commonly used nanomaterials in our health care system for hundreds of years. Recently, Ag NPs have become of intense interest in biomedical applications, because of their antibacterial, antifungal, antiviral, and anti-inflammatory activity (El-Badawy et al., 2010).

The aim of this study is to evaluate the efficacy of CCNPs and Ag NPs as a bone graft substitutes in repairing of an experimentally induced segmental bone defects through radiographic.

MATERIALS AND METHODS

Animal model and housing

Twenty-four adult apparently healthy New Zealand White rabbits aging from five to six months and weighting 3.5 ± 0.5 kg were used in this study. All rabbits were free from systemic and musculoskeletal disorders. The rabbits were housed singly or in pairs in stainless steel cages with an area of 0.36 cm^2. All rabbit kept in humidity 55-60% with 12 hours light/dark cycle and temperature 25 (±3) °C. they had free access to standard diet and water adlibtum during the whole of experiment. The protocol was approved by the Animal Care and Use Committee, University of Sadat City – faculty of Veterinary Medicine, Sadat City, Egypt.

Preparation of bone substitutes

The nanoparticles (which used in this study) were synthesized in Nanomaterials synthesis and research unit, Animal Health Research Institute (AHRI), Agriculture Research Centre (ARC), Egypt.

A. preparation of CCNPs powder:

1. The coral fingers (*porites sp.)* were cut onto small pieces and each part was rasped to remove any suspended impurities.
2. The coral fingers were crushed into small particles (with diameter 0.5 – 1 mm).

According to Hussein et al. (2020): 5g of coral powder was dissolved into 20 mL of 5M (42ml) hydrochloric acid (HCl) 37%, Emsure® (Merck KGaA, Darmstadt, Germany) to form calcium chloride ($CaCl_2$). The solution was filtered with filter papers (Filters Fioroni Filter Circles 70 mm, Lab Logistic Group GmbH, Meckenheim, Germany). Contamination products were extracted from the solution using an electric mixer spun at 500 rpm for 1 h at room temperature.The formed $CaCl_2$ was then diluted with 1 L double distilled water (DDW) to form stock solution. Stock solution of K_2CO_3 was prepared by dissolving 5 g of K_2CO_3 ACS reagent, 99% (Sigma Aldrich, Steinheim, Germany) in 100 mL of DDW.50ml of DDW were then added to 10 mL of diluted $CaCl_2$ followed by the addition of 10 mL of diluted K_2CO_3 at 1hr drop wise. The solutions were then left for 24 h to precipitate. Then, the supernatant solution was discarded and the resultant product was centrifuged at 6000 rpm for 15 min. The acidity of the resultant solution was then neutralized by washing three times with DDW. The resultant product was either dried using a hot oven at 110 ℃ for 24 h.

Preparation of CCNPs paste:

The technique was performed on the same basis as mentioned Saraswathy et al., (2004).

1. 1.5 g Gelatin was dissolved in 3 ml Hcl (N: 0.1) in water bath at 55 °C.
2. The CCNPspowder were added to the previously prepared mixure and made into paste.
3. The paste was filled in a plastic syringe of 1 ml capacity after cutting the narrow end.
4. The extruded paste was cut into the require length and allowed to cure overnight in the room temperature.
   The prepared pastes were packed in double wrapped plastic roll and sterilized by ultraviolet light for 30 second just before operation.

Preparation of AgNPs:

According to **Amer, et al., (2018):** 50 ml of 0.002 M AgNO3 (0.01698g) in de ionized water was heated to boil. To this solution 5 mL of 2 % tri sodium citrate (0.1g) was added drop by drop. During the process, solutions were mixed vigorously and heated until change of color was evident (grayish yellow). Then it was removed from the heating device and stirred until cooled to room temperature. Centrifuge at 10000 rpm for 15 min. and wash three times with DDW, re disperse pellet in deionized water.

Preparation of CCNPs/AgNPS paste:

As the same steps of CCNPs paste preparation with adding 5 ml of AgNPs to the mixture.

Characterization of prepared nanoparticles

The particles size and surface charge of prepared NPs were characterized using a Malvern Zetasizer ZS-series (DLS, Malvern Co, UK). Thereafter, the morphological investigation of synthesized-NPs was detected by Transmission Electron Microscopy (TEM) (JEM-2100, JEOL). Phase identification and crystalline structure of CaCO3 NPs were performed by using X-Ray Diffractometer, XRD (SHIMADZU, XRD-6000) with Cu Ka radiation. The concentration of Ag NPs was quantitatively measured by ICP-MS instrument (Elan DRC-e, PerkinElmer, Germany).

1. Calcium Carbonate nanoparticles (CCNPs)

1.1. X-Ray diffraction (XRD)

Figure (1) shows the XRD analysis of the composition and phase of the optimized CaCo3 NPs derived from coral. The presence of CCNPs can be observed at 2θ of 23.0, 29.5, 36.0, 39.4, 43.2, 47.5, 48.5, 57.4, 60.7, 63.1, 64.6, and 65.6◦. The assignments of 2θ position and other parameters for CCNPs from XRD were in agreement with the reference code 2100189 of a hexagonal crystal system and space group R-3c. The formation of the calcite phase of CaCo3 in the current investigation matched well with the results of Kontoyonis et al. (2000) with the characteristic peak positioned at 2θ = 29.5◦ at wave length of 1.54060. (Fig.1)

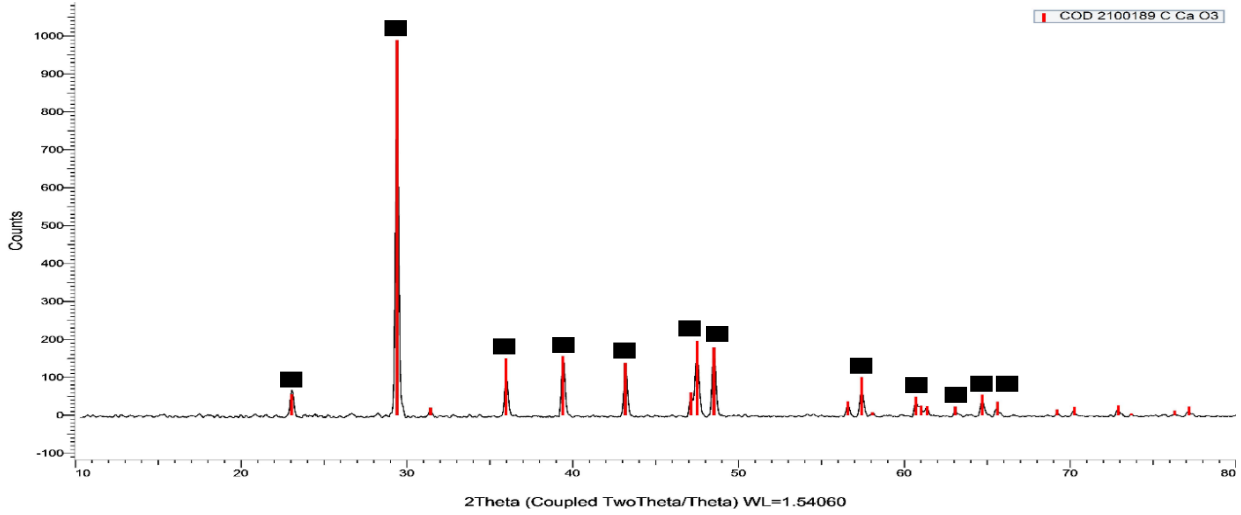

Fig. (**1):** XRD analysis of CCNPs.

1.2. Dynamic Light Scattering (DLS) examination:

The results of DLS showed that the average particle size of CaCO3 NPs is 88.4 nm with poly dispersity index (PDI) of 0.4 and surface charge of -17.3 mv. (Fig. 2)

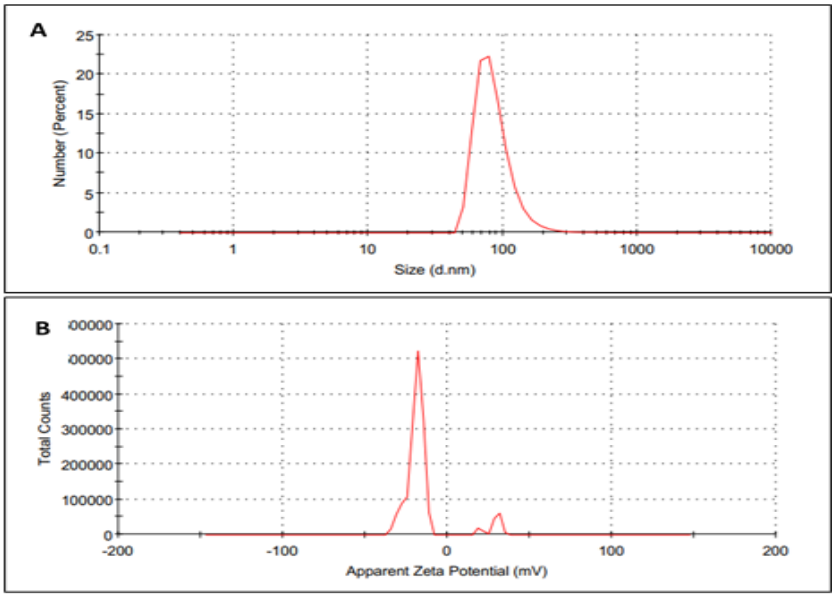

Fig. (2): DLS examination of CCNPs, (A) is particle size distribution (nm) by number, (B) is apparent zeta potential (mv).

1.3. Transmission Electron Microscope (TEM) examination

TEM imaging of CCNPs showed monodisperse, un agglomerated nano spheres with particle size ranged from 11.3-15 nm (Figure.3).

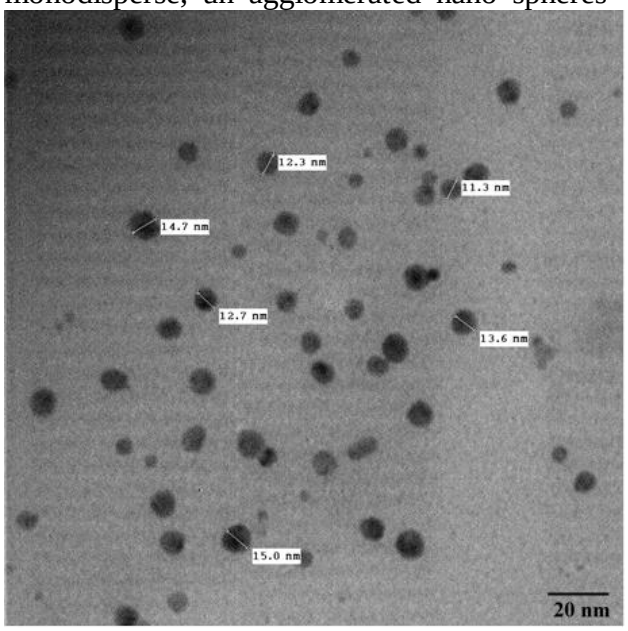

Fig. (3): TEM examination of CCNPs showed monodisperse, un agglomerated nano spheres with particle size ranged from 11.3- 15 nm. Scale bar is 20 nm.

2. Silver nanoparticles (AgNPs)

2.1. DLS examination

The results of DLS showed that the average particle size of Ag NPs is 10.4 nm with poly dispersity index (PDI) of 0.4 and surface charge of -31.3 mv. (Fig. 4).

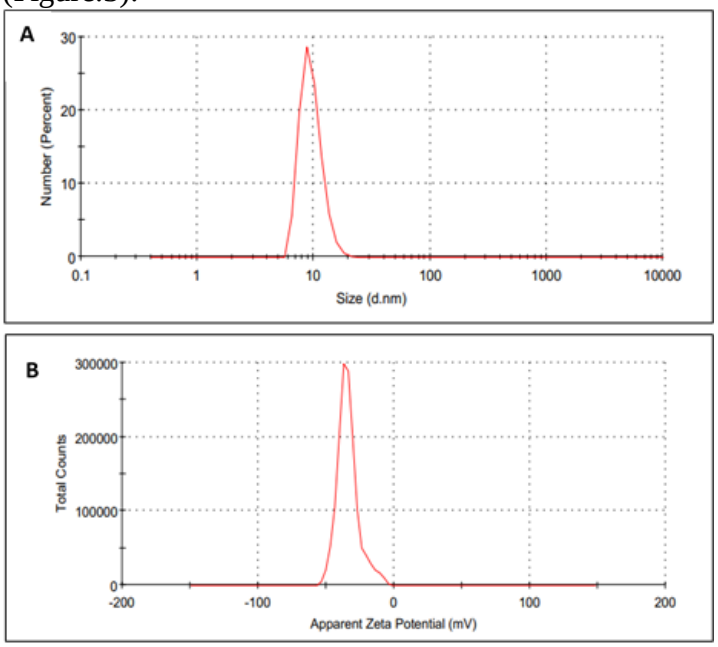

Fig. (4): DLS examination of AgNPs, (A) is particle size distribution (nm) by number, (B) is apparent zeta potential (mv).

2.2. Transmission Electron Microscope (TEM) examination

TEM imaging of Ag NPs showed ultrafine uniform, well dispersed spherical nanoparticles with particle size ranged from 2.79- 4.44 nm (Fig. 5).

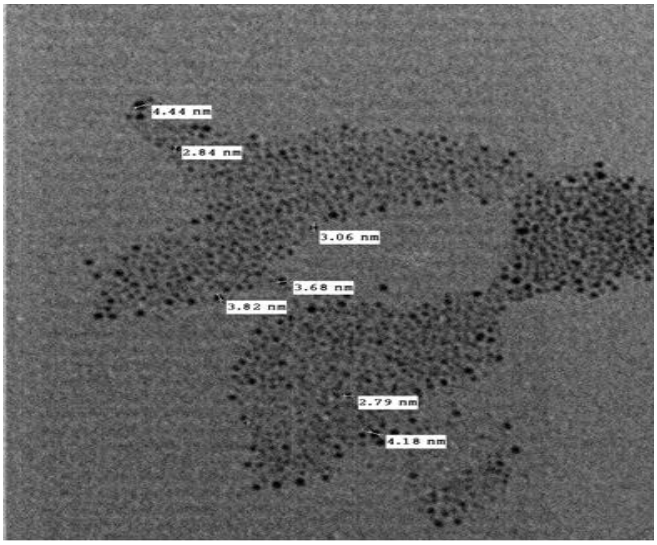

Fig. (5): TEM examination of Ag NPs showed ultrafine uniform well dispersed spherical nanoparticles with particle size ranged from 2.79- 4.44 nm. Scale bar is 20 nm.

2.3. Determination of AgNPs concentration

Silver concentration was detected using ICP-MS, the silver concentration was 12.247 mg/l.

Surgical technique:

A prophylactic dose of antibiotic of Enrofloxacin (Curabiotic®: CureVet Co.; A.R.E) at dose 5 mg/kg body weight was administered I/M before surgery by about 30 minutes. The anteriomedial aspect of lower region of right forelimb was clipped, shaved, washed and scrubbed with antiseptic (Betadine®).All animals were anesthetized by intramuscular administration of 40 mg/kg ketamine hydrochloride **(**KETALITE®: ELICE Pharma; Pakistan) and 5 mg/kg xylazine Hcl (Xylaject®: 2% sol. ADWIA Co., A.R.E). All rabbits restrained in sternal recumbency.

Surgical approach and biomaterials implantation:

A 5-cm skin incision was made craniomedially over the forelimb.The radius was exposed by dissecting the surrounding muscles.A 14-mm critical-sized defect (Zhao et al., 2016) was then created in the diaphysis of the right radius.The defect of the animals in the group (A) the bone defect was filled with CCNPs paste only. In the group (B) the bone defect was filled with CCNPs/AgNPs paste. The muscles and subcutaneous tissue were closed using simple continuous pattern.

After surgery an X-rays image was taken to record the day zero, a prophylactic dose of antibiotic of Enrofloxacin (Curabiotic®: CureVet Co.; A.R.E) at dose 5 mg/kg body weight for three successive days, and stiches was removed after 7 days.

Radiographic evaluation

The sequence of bone healing in terms of filling of the segmental defects with bone deposition was monitoring via sequential radiographs taken immediately post operation and at 2nd, 4th, 8th, 12th week of observation period. An X-rays apparatus (semens 300) was used to take mediolateral view at 45 KV, 30 mAs and 80 cm FFD.The radiographic images were evaluated by two radiologists (without previos information), The radiographs were scored using Modified Lane–Sandhu scoring system (Parizi et al., 2013) (Table 1).

Table (1): Modified Lane–Sandhu radiographic scoring standard by Parizi et al. (2013):

Item		score
Bone formation	No evidence of bone formation	0
	Bone formation occupying 25% of the defect	1
	Bone formation occupying 50% of the defect	2
	Bone formation occupying 75% of the defect	3
	Bone formation occupying 100% of the defect	4
Union (proximal and distal ends were evaluated separately)	No union	0
	Possible union	1
	Radiographic union	2
Remodeling	No evidence of remodeling	0
	Remodeling of medullary canal	1
	Full remodeling of cortex	2
Total points possible per	Bone formation	4

category	Proximal union	2
	Distal union	2
	Remodeling	2
	Maximum score	**10**

Statistical analysis:

All the results were reported as mean, median and standard deviations. A one-way ANOVA was used to carry out statistical analysis. $p \leq 0.05$ was considered as statistically significant. All the values were analyzed using the SPSS software (version 20.0; IBM, America).

RESULTS

There were no infections or any complications observed in all operated cases along the observation period.Radiographically, in our study, the radiographic imaging showed that adding bone graft substitutes to critical segmental radial defect with length 14 mm have great radiographic changes (fig. 7&8).

Bone formation scoring revealed significant difference between group A and group B only at the end of observation period (P=0.017), while there was a highly significant difference in the CCNPs group and CCNPs/Ag NPs group at all time points (P=0.00-0.001).

proximal cortical union scoring revealed significant difference between group A and group B only at the end of observation period (P=0.017). There was a highly significant difference in the CCNPs/Ag NPs group at all time points (P=0.001), whileThere was a highly significant difference in the CCNPs group at all time points (P=0.33).

distal cortical union scoring revealed no significant difference between group A and group B along the observation period (P=0.347-1.0), while there was a highly significant difference in the CCNPs group and CCNPs/Ag NPs group at all time points (P=0.00-0.001).

bone remodeling appeared in group A at the end of observation period while in group B appeared in the 8th week post-operation. Bone formation scoring revealed significant difference between group A and group B only at the end of observation period (P=0.017).

The total radiographic score revealed no significant difference between CCNPs group and CCNPs/Ag NPs group at the first two observation periods (2nd and 4th) post-operative weeks, while at the 8th and 12th post-operative weeks there was significant difference (P= 0.043-0.018) respectively.

Table (2): Showing bone formation score between groups A&B:

Groups	**Times (weeks)**					**P-value**
	Zero	**2w**	**4w**	**8w**	**12w**	
CCNPs	0 (0.0-0.0)^{c}	0 (0.0-0.0)^{c*}	1 (1.0-1.0)^{b*}	2 (1.0-2.0)^{b*}	3 (2.0-3.0) ^{a*}	**0.001**
CCNPs/Ag NPs	0 (0.0-0.0)^{d}	0 (0.0-0.0)^{d*}	1 (1.0-2.0)^{c*}	2 (2.0-3.0)^{b*}	4 (3.0-4.0)^{a**}	**0.000**
p. value	**-**	**1.0**	**0.195**	**0.141**	**0.017**	

Table (3): Showing proximal cortical union score between groups A&B:

Groups	**Times (weeks)**					**P-value**
	Zero	**2w**	**4w**	**8w**	**12w**	
CCNPs	0 (0.0-0.0)^{a}	0 (0.0-0.0)^{a*}	1 (0.0-1.0)^{a*}	1 (0.0-1.0)^{a*}	1 (0.0-1.0)^{a*}	**0.330**
CCNPs/Ag NPs	0 (0.0-0.0)^{c}	0 (0.0-0.0)^{c*}	1 (1.0-1.0)^{b*}	1 (1.0-1.0)^{b*}	2 (1.0-2.0)^{a**}	**0.001**
p-value	**-**	**-**	**0.195**	**0.347**	**0.040**	

Table (4): Showing distal cortical union score between groups A&B:

Groups	**Times (weeks)**					**P-value**
	zero	**2w**	**4w**	**8w**	**12w**	
CCNPs	0 (0.0-0.0)^{c}	0 (0.0-0.0)^{c*}	1 (1.0-1.0)^{b*}	1(1.0-2.0)^{a,b*}	2 (1.0-2.0)^{a*}	**0.001**

CCNPs/Ag NPs	0 (0.0-0.0)^{c}	0 (0.0-0.1)^{c*}	1 (1.0-1.0)^{b*}	2 (1.0-2.0)^{b*}	2 (2.0-2.0)^{a*}	**0.000**
p-value	**-**	**0.347**	**1.0**	**0.347**	**0.347**	

Table (5): showing Remodeling score between group A&B:

Groups	**Times (weeks)**					**P-value**
	zero	**2w**	**4w**	**8w**	**12w**	
CCNPs	0 (0.0-0.0)^{b}	0 (0.0-0.0)^{b}	0 (0.0-0.0)^{b}	0 (0.0-0.0)^{b*}	1 (0.0-1.0)^{a*}	**0.034**
CCNPs/Ag NPs	0 (0.0-0.0)^{c}	0 (0.0-0.0)^{c}	0 (0.0-0.0)^{c}	1 (0.0-1.0)^{b**}	1 (1.0-2.0)^{a**}	**0.004**
p-value	**-**	**-**	**-**	**0.081**	**0.017**	

*,**:Medians and ranges with different asterisks superscripts in the same column are significantly different at P<0.05.

a,b,c,d: Medians and ranges with different small superscripts letters in the same row are significantly different at P<0.05.

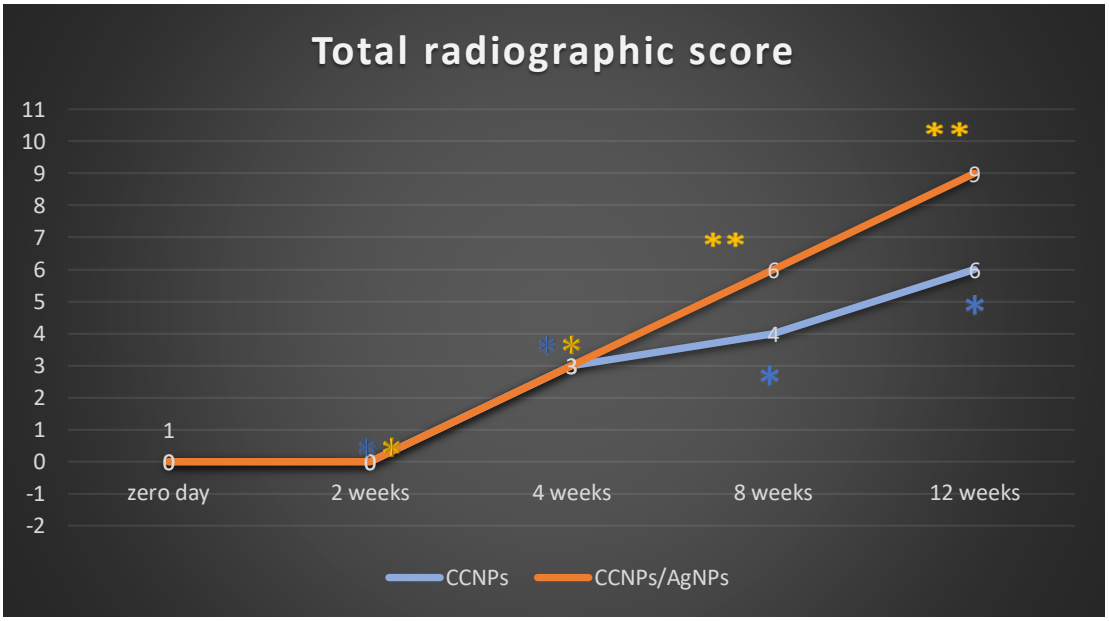

Fig. (6): The total radiographic score revealed no significant difference between CCNPs group and CCNPs/Ag NPs group at the first two observation periods(2nd and 4th) post-operative weeks, whileat the 8th and 12th post-operative weeks there was significant difference (P= 0.043-0.018) respectively. *,**:Medians and ranges with different asterisks superscripts in the same time period are significantly different at P<0.05.

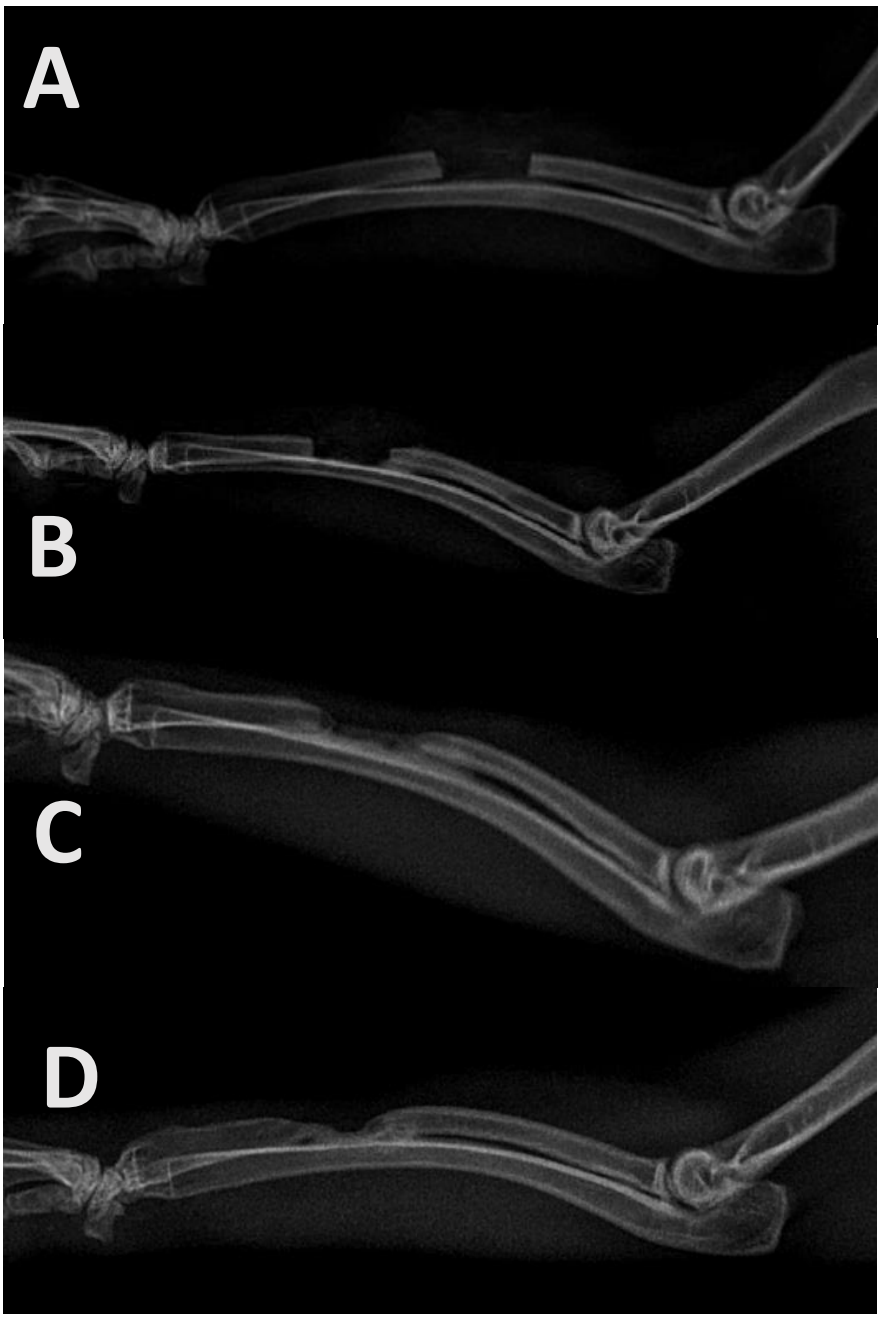

Fig. (7): showing radiographic images of CCNPs group at 2nd week (A), 4th week (B), 8th week (C) and 12th week (D).

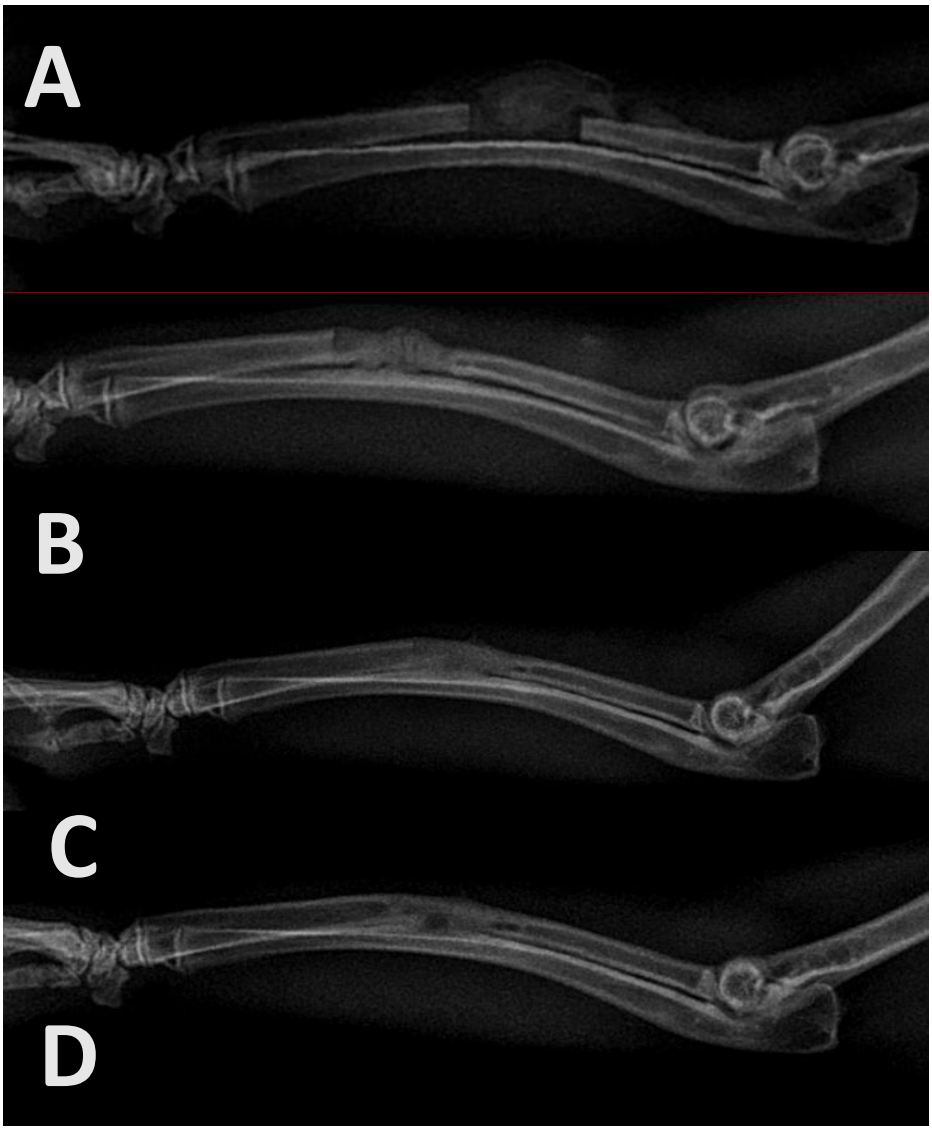

Fig. (8): showing radiographic images of CCNPs/Ag NPs group at 2nd week (A), 4th week (B), 8th week (C) and 12th week (D).

DISCUSSION

This study was aimed to evaluate the efficacy of CCNPs and Ag NPs as a bone graft substitutes in repairing of an experimentally induced segmental bone defects.There are no infections or any complications observed in all of operated animals.

Critical size defect (CSD) is defined as the smallest size of the intraosseous wound in a particular bone and species of animal which shows less than 10% spontaneous healing during the lifetime of the animals (Zhao et al., 2011). In present study, a critical size segmental defects (14 mm) were artificially induced in rabbit's radius. This is agreement with those reported by (Zhao et al., 2016) who indicates that in order to be critical sized, defects must be greater than 1.4 cm when using rabbit radial defect model involving 6-month-old healthy New Zealand white rabbits. The rabbit's forelimbs are Supported by the intact ulna without need for internal fixation following middle radial defects.

Radiologically, in CCNPs group, complete resorption of CCNPs paste had occurred but there were not high rates of new bone formation to bridge the gap in any animal, although some new bone formation, the bone marrow cavity (canalization) was not formed in all animal. This data agreed with (Meng et al., 2019) when they use α- calcium sulfate hemihydrate to reconstruction segmental radial defect in rabbits, but disagreed with (Parizi et al., 2012) as they reported complete union when they used coral powder to fill segmental radial defect, this is may be due to small defect size in their study (10 mm) which considered non CSD.

CCNPs paste was absorbed very quickly in which radiographic images showed any traces of CCNPs at four weeks post operation and this hinders rapid healing. This data disagreed with data which reported by (Maleki et al., 2015) who mentioned that CCNPs has low biodegradability in their invitro study.

AgNPs had gained attention due to their exclusive biological, chemical, and physical properties in comparison to their large size equivalents. As any nano material celltoxicity should be considered. A further study by Necula et al., (2012) focused on the in vitro cytotoxicity of silver nanoparticles of various concentrations using a human fetal osteoblastic cell line and evaluated their bactericidal activity against MRSA. The results showed that high concentrations of silver nanoparticles (3000 mg/l Ag) were extremely cytotoxic, but lower concentrations (300 mg/l Ag) demonstrated optimum cell growth of osteoblasts as well as good antibacterial properties. In our study, the AgNPs concentration was 12.24 mg/l.

Addition of AgNPs to CCNPs in group B improved the efficacy of the graft in which the defect was filled with new bone with signs of remodeling (score=1) at the end of observation period. The biodegradability of CCNPs decreased, this is an agreement with (Morley et al., 2007) as they found that addition of AgNPs to ultra-high-molecular-weight polyethylene for fabricating inserts for total joint replacement components, could drastically reduced the wear and tear of the polymer.Also the antimicrobial effect of AgNPs is associated with improved clinical outcomes without the need for long courses of intravenous antibiotics (Nair, 2008).

In this study adding AgNPs in group B could accelerate bone regeneration and new bone formation. These data agreed with Zhang et al., (2015) as the found that that AgNPs could promote the formation of the fibrous joint and the subsequent end joining of the fracture bone via multiple routes: chemoattraction of MSCs and fibroblasts to migrate to the fracture site, induction of the proliferation of MSCs and fibroblasts, and induction of osteogenic differentiation of MSCs. It may be possible that AgNPs also promote the proliferation and differentiation of the fibroblasts adjacent to the fracture site to form the granulation tissue and the fracture callus. In addition, the cells in the fracture callus expressed TGF-β1 and phosphorylated SMAD5, which indicated that AgNPs induced and activated TGF-β/BMP signaling in these cells (Liu et al., 2010).

CONCLUSION

CCNPs has limited efficacy in bone generation when it has been used alone.Addition of AgNPs to CCNPs improves its efficacy when used to fill a critical segmental defect in rabbits.Further animal studies and trials are now needed to further investigate the bone generation potential of CCNPs and AgNPs.

REFERENCES

Amer, S. A., Nouh, S. R., Elkammar, M. H., Shalaby, T. I., &Korittum, A. S. (2018): Silver Nanoparticles Preparation and their Effect on Full-thickness Skin Wound Healing in Rabbit Model. Alexandria Journal for Veterinary Sciences, 57(2).

Castro, P., Huber, M.E. (2008): Marine biology. Boston: McGraw-Hill Higher Education.

Chen, J., Ouyang, J., Kong, J., Zhong, W., Xing, M.M., (2013): Photo-cross-linked and pH-sensitive biodegradable micelles for doxorubicin delivery. ACS Appl Mater Interfaces.;5(8):3108–3117.

El-Badawy, A., Feldhake, D., Venkatapathy, R., (2010): State of the Science Literature Review: Everything Nanosilver and More. Washington, DC: US Environmental Protection Agency.

Esposito, M., Grusovin, M.G., Rees, J., Karasoulos, D., Felice, P., Alissa, R., Worthington, H., Coulthard, P. (2010): Effectiveness of sinus lift procedures for dental implant rehabilitation: a Cochrane systematic review. European Journal of Oral Implantology 3:7–26.

Hak, D.J., Fitzpatrick, D., Bishop, J.A., Marsh, J.L., Tilp, S., Schnettler, R., Simpson, H., Alt, V., (2014): Delayed union and nonunions: epidemiology, clinical issues, and financial aspects, Injury 45 (Suppl. 2) (2014) S3–S7.

Hussein, A. I., Ab-Ghani, Z., Che Mat, A. N., Ab Ghani, N. A., &Husein, A. (2020): Synthesis and Characterization of Spherical Calcium Carbonate Nanoparticles Derived from Cockle Shells. Applied Sciences, 10(20), 7170.

Kontoyannis, C.G.; Vagenas, N.V., (2000): Calcium carbonate phase analysis using XRD and FT-Raman spectroscopy. Analyst, 125, 251–255.

Liu, X., Lee, P.Y., Ho, C.M., Lui, V.C., Chen, Y., Che, C.M., Tam, P.K& . Wong, K.K., (2010): Silver nanoparticles mediate differential responses in keratinocytes and fibroblasts during skin wound healing. ChemMedChem 5, 468-475.

Mahmood, S.K., Razak, I.A., Ghaji, M.S., Yusof, L.M., Mahmood, Z.K., Rameli, M.A.B.P., Zakaria, Z.A.B., (2017): In vivo evaluation of a novel nanocomposite porous 3D scaffold in a rabbit model: histological analysis. Int J Nanomedicine. Dec 1;12:8587-8598.

Meng, Z.L., Wu, Z.Q., Shen, B.X., et al., (2019): Reconstruction of large segmental bone defects in rabbit using the Masquelet technique with α-calcium sulfate hemihydrate. J Orthop Surg Res 14, 192.

Mohamed, A., Xing, M.M., (2012): Nanomaterials and nanotechnology for skin tissue engineering. Int J Burns Trauma.;2(1):29–41.

Parizi, A.M., Oryan, A., Shafiei-Sarvestani, Z., Bigham-Sadegh, A. (2013): Effectiveness of synthetic hydroxyapatite versus Persian Gulf coral in an animal model of long bone defect reconstruction. J OrthopaedTraumatol; 14:259–268

Puska M., Aho, A.J., Vallittu, P.K., (2013): Biomaterials in bone repair, Duodecim 129.496–489

Zhang, R., Lee, P., Lui, V., Chen, C.H.; Liu, X., Lok, Chun., N., Michael, Yeung, W.K., Wong, K.Y., (2015): Silver nanoparticles promote osteogenesis of mesenchymal stem cells and improve bone fracture healing in osteogenesis mechanism mouse model. Nanomedicine: Nanotechnology, Biology and Medicine, S1549963415001598.

Zhao, M. D., Huang, J. S., Zhang, X. C., Gui, K. K., Xiong, M., Yin, W. P., Yuan, F. L., & Cai, G. P. (2016): Construction of Radial Defect Models in Rabbits to Determine the Critical Size Defects. PloS one, 11(1), e0146301.

Zhao, M., Zhou, J., Li, X., Fang, T., Dai, W., Yin, W., et al., (2011): Repair of bone defect with vascularized tissue engineered bone graft seeded with mesenchymal stem cells in rabbits. Microsurgery 31: 130–137.